proceedings

MDPI

Type of the Paper (Proceeding)

The effect of loading rate on the mode I interlaminar fracture toughness†

Huifang Liu [1, 2], Chao Zhang [1, 2] and Yulong Li [1, 2,*]

[1] School of Aeronautics, Northwestern Polytechnical University, Xi'an, 710072, China
[2] Shaanxi Key Laboratory of Impact Dynamics and Its Engineering Application, Northwestern Polytechnical University, Xi'an, 710072, China
Emails: fenghuang1108@163.com, chaozhang@nwpu.edu.cn, liyulong@nwpu.edu.cn
* Correspondence: liyulong@nwpu.edu.cn; Tel.: +86-029-88494859

† Presented at the 18th International Conference on Experimental Mechanics, ICEM18, Brussels, 2018
.

Published:

Abstract: This paper studies the effect of loading rate on mode I interlaminar fracture of unidirectional carbon/epoxy laminates. Double cantilever beam (DCB) test geometry was used to test quasi-static and dynamic fracture toughness. The DCB specimens were loaded symmetrically by a novel electromagnetic Hopkinson bar system at the maximum loading rate 30 m/s. The crack initiation is monitored by a pair of strain gage mounted on the surface of DCB arms. The hybrid experiment-numerical methods was used to calculate the fracture toughness by employing J-integral technique for quasi-static and dynamic tests. The finite element model takes use of incident stress wave as the boundary conditions for dynamic tests. It shows that the fracture toughness is rate positive at high loading rates, and rate insensitive at low loading rates.

Keywords: Polymer-matrix composites; Delamination; Dynamic fracture, Rate effect

1. Introduction

Delamination is the one of the predominated damage modes in fiber-reinforced polymer composites. The growth of delamination results in significant stiffness degradation. The composites are easily to delaminate due to insufficient interlaminar strength, especially subjected to low and high velocity impact, such as tool drop, hail and bird impact. Thus, the study of loading rate effect on the interlaminar crack is essential in the design and analysis of composite structure.

Numerous investigations have been conducted on understanding the rate effect on mode I delamination fracture toughness of PMCs in recent years, and the strain rate dependency can either increase, decrease and be independent of loading rate [1]. This inclusive results about the rate dependency of interlaminar fracture toughness may be attributed to materials property and different test setups.

Different sample geometries and loading methods has been used to study the loading rate effect. DCB test is of particular interest to measure dynamic interlaminar fracture toughness since it is the standard test geometry under quasi-static conditions. One of the main challenges arising as the loading rate increases is to keep symmetrical opening of the DCB specimen which make sure pure mode I interlaminar fracture [2] and also reduce the vibration of the specimen.

Several experimental methods have been proposed to ensure symmetric opening when loading rate is high. One setup is proposed by Hug [3] which translate low vertical displacement of cross-head to high horizontal opening using lever principle. The maximum loading rate (about 3 m/s) is refrained by the inertia effect of the loading apparatus. And several researchers use drop tower to wedge impact the DCB specimen. This method suffers from friction which results in strong

oscillations and the maximum loading rate is 3 m/s. However, the symmetrical loading rate over 10 m/s is not yet within sight.

In this paper, DCB specimens is symmetrically loaded by a dual electromagnetic Hopkinson under dynamic loading with maximum loading rate 30 m/s. The quasi-static tests used universal test machine at the loading rates 0.08 mm/s. Under dynamic loading conditions, the crack initiation is monitored by strain gage mounted on the DCB arms. The fracture toughness is calculated is determined by a hybrid experimental-numerical method.

2. Materials and Methods

3.1. Mterials and specimens

The unidirectional panels were fabricated from Cytec™ T700/MTM28-1 carbon fiber prepreg according to the manufacturer's specifications. The starter crack was introduced in the mid-plane with a 13 μm thick non-adhesive PTFE film (Teflon). One unidirectional plate was cured: [0_{16}/Teflon/0_{16}], corresponding to the thicknesses 4 mm. The fiber volume fraction and density of the laminates are 61% and 1522 kg/m3. The material properties is listed in Table 1. The geometry of DCB specimen for quasi-static test is shown in Figure 1. The dynamic DCB specimens includes several initial crack lengths: 60 mm, 40 mm, 32 mm and 20mm.

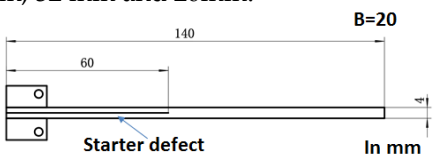

Figure 1. Schematics of the DCB specimens for quasi-static tests.

Table 1. Material properties of the unidirectional T700/MTM28-1 carbon/epoxy.

E_{11} (GPa)	E_{22} (GPa)	E_{33} (GPa)	G_{12} (GPa)	G_{13} (GPa)	G_{23} (GPa)	ν_{12}	ν_{13}	ν_{23}
127	8.4	8.4	3.7	3.7	3.28	0.3	0.3	0.45

3.2 Quais-static experiment

The quasi-static DCB tests were performed in an Instron 5848 equipped with 100N load cell, according to the standard ASTM 5528 [4]. The crosshead displacement rate, 0.08mm/s, was chosen. The specimens were loaded to crack initiation. The load P and opening displacement δ were recorded at sample rate 100 Hz.

3.3 Dynamic experiment

Figure 2(a) shows the schematic of dynamic DCB test setup using the dual electromagnetical Hopkinson bar. The operation principle of the apparatus is described in detail in [5]. The stress wave is generated by electromagnetic induction. Through a parallel connection of active coils, dual synchronized incident stress waves are then generated in the two incident bars. The parameters of the Hopkinson bar test is shown in Table 2. The DCB specimen and the incident bars were connected through hinges, as shown in Figure 2(b). Two pairs of strain gages (SG-1 and SG-2) were mounted on the two incident bars to record the incident (ε_i) strain signals, as shown in Figure 2. And the distance between the strain gage and loading point is d_1. Two strain gages (DCB-1and DCB-2) are attached on the surface of DCB arms. Two crack-propagation gages are attached on the edge of DCB specimen to monitor the propagation of the dynamic crack.

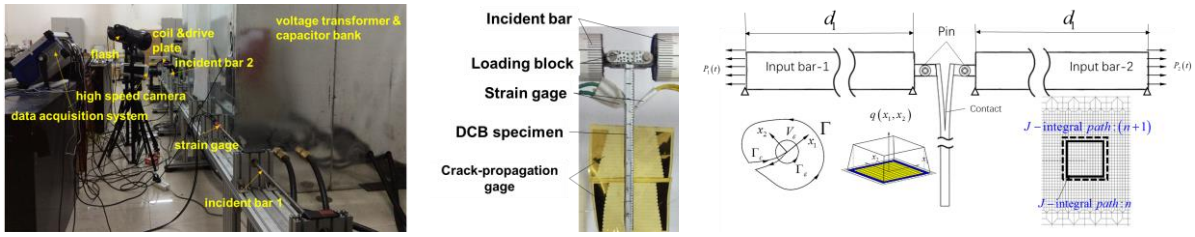

(**a**) (**b**) (c)

Figure 2. (**a**) Schematic of dynamic test using electromagnetic Hopkinson bar; (**b**) Schematics of DCB; (**c**) Schematics of finite element model for dynamic test, and the insert is integral contour.

Table 2. Parameters of the electromagnetic Hopkinson bar.

E (GPa)	ρ (kg/m^3)	D (mm)	L_{Inp} (m)	d_1 (m)	C_0 (m/s)
105.8	4500	18	3.5	2.1	4849.54

3.4. Hybrid experimental-numerical method

Figure 3 shows the schematics of the numerical model and corresponding fracture toughness calculation methods for the DCB test. Four-node plane strain element with reduced integration (CPE4R) is used in FEM models. Explicit time integral was used for the dynamic simulations, while standard implicit time integral was used for the quasi-static simulations. The DCB specimen is considered as an orthotropic body with linear-elastic properties listed in Table 1. The finite element mesh was refined with an element size of 10 μm to ensure stress convergence. Tied constrain was used to connect the loading blocks and the DCB specimen. Hard contact with no friction was defined between the initial crack surfaces.

Under quasi-static conditions, the opening displacement was used as boundary condition. While under dynamic conditions, the incident stress wave signals ($P_1(t)$ and $P_2(t)$) is employed, as shown in Figure 3. The model includes the Hopkinson bars, piano hinges and loading pins. The length of input bar is d_1. The material prperties of the input bar are listed in Table.2. The width of the Hopkinson bar was simplified as A_{inc}/B, where A_{inc} is the area of the Hopkinson pressure bar, and B is the width of the DCB specimen. The poison ratio is set to zero to obtain the same elastic wave speed with experiment for plane strain model. This simplification did not result in significant deviation due to the wave propagation properties of unidirectional polymer composites. The interaction between piano hinge and loading pin is hard contact without friction due to lubrication.

For dynamic loading conditions, the dynamic J-integral was adopted to calculate ERR, which is written as:

$$J_k^d = \int_{\Gamma+\Gamma_c} \left((W+K)n_k - t_i \frac{\partial u_j}{\partial x_k} \right) d\Gamma + \int_{V_\Gamma - V_\varepsilon} \left((\rho \ddot{u}_i - f_i) \frac{\partial u_i}{\partial x_k} - \rho \frac{\partial \dot{u}_i}{\partial x_k} \dot{u}_i \right) dA \qquad (1)$$

where u_i, t_i, f_i, n_k and ρ denote the displacement, traction, body force, outward normal direction and density, respectively. W is the strain-energy density, K is the kinetic-energy density. Γ, Γ_ε and Γ_c denote the far-field, near-field and crack surface paths, respectively. V_Γ is the area encircled by far-field path Γ, and V_ε is the region surrounded by Γ_ε. For quasi-static fracture, the static J-integral is calculated by setting the second part of Eq. (1) to zero. For quasi-static model, the ERR is calculated by setting the second part of Eq. (1) to zero.

The line integral of Eq. (1) is not feasible for finite element calculation, which is transferred to domain integral based on divergence theorem by introducing a weight function q. It has been shown that if the function q is sufficiently smooth, the shape of the function has little influence on the integration value. All implementations in this paper use a linear function of q with a value between zero and one, as shown in Figure 4. The J-integral was calculated using a separately written Python program which used the domain integral method.

3. Results and Discussion

3.1. Quasi-static experimental results

Figures 4(a) shows the typical load-deflexure curves under 0.08 mm/s loading rate. And Figure 4(b) compares the ERR evolutions obtained by hybrid experimental and numerical model using different crack tip element size. It shows that the hybrid method is mesh independent.

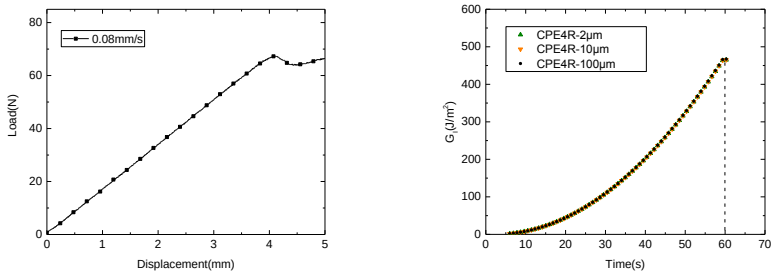

(**a**) (**b**)

Figure 3. (**a**) Typical loading-displacement curve at 0.08mm/s opening displacement rates; (**b**) the ERR calculated using different mesh size.

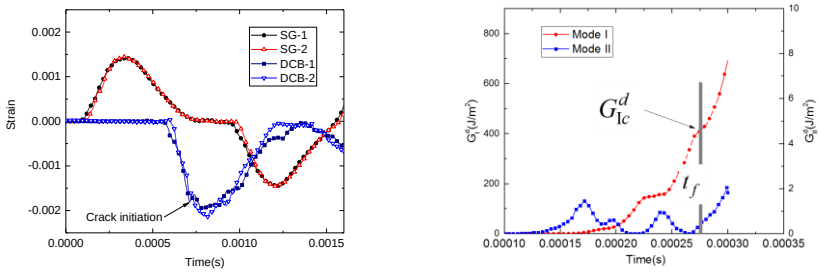

(**a**) (**b**)

Figure 4. (**a**) Typical signals from Hopkinson bars (SG-1~SG-2), strain gage mounted on the arm surface (DCB-1 and DCB-2) for specimen ($2h$ = 4 mm, a_0 = 40 mm, L = 100 mm); (**b**) Mode I and II energy release rate calculated by dynamic J-integral.

3.2 Dynamic experimental results

The electromagnetic Hopkinson bar was used to load the DCB specimen under dynamic condition. The original signals include two strain gages on the incident bars (SG-1~SG2), two strain gages on the surface of DCB arms (DCB-1 and DCB-2), as shown in Figure 5(a). Figure 5(b) shows the mode I and II ERR evolutions. It is clear that the mode II ERR is close to zero which implies that pure mode I interlaminar fracture was kept during dynamic loading. When crack initiates under dynamic loading, there is a sudden drop in strain signals DCB-1 and DCB-2, the crack initiation time is then determined. The fracture toughness is then determined as the critical value ERR at crack initiation.

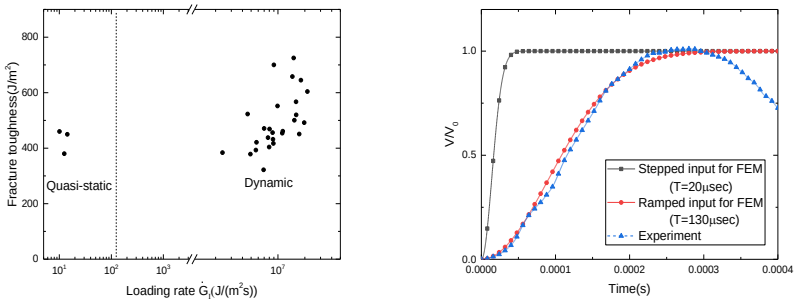

(a) **(b)**

Figure 5. (**a**) Loading rate dependency of Mode I interlaminar fracture toughness; (**b**) Time histories of particle velocity of the loading point with various rising time.

3.3 Dynamic effect

To reveal the dynamic effect on the deformation of DCB specimen, numercial analysis was carried out by using the following opeing velocity:

$$\dot{\delta}(t) = V_0\left(1-(t/T)^2\right) \tag{2}$$

where T is a rise-time parameter. The typical experimental incident wave was plotted in Figure 5(b). When T is 130 μs, the opeing rate is ramped (equals to dynamic test) and T is 20 μs, the opeing rate is stepped. Besides hybrid method, the compliance method is also used to calculate the ERR [3]:

$$G^d_{\mathrm{I-Compliance}} = \frac{3}{16}\frac{E_1 h^3 \delta^2}{\left(a+\Delta_I\right)^4} - \frac{33}{560}\rho h\dot{\delta}^2 \tag{3}$$

where δ is opening displacement, Δ_I is mode I crack length correction, ρ is the density of composites and $\dot{\delta}$ is displacement rate.

The difference betweeb ERRs calculated from compliamce and hybrid method is shown in Figure 6(a). As shown in the figure, the compliance method underestimates the energy release rate significantly, especially when displacement rates are high.

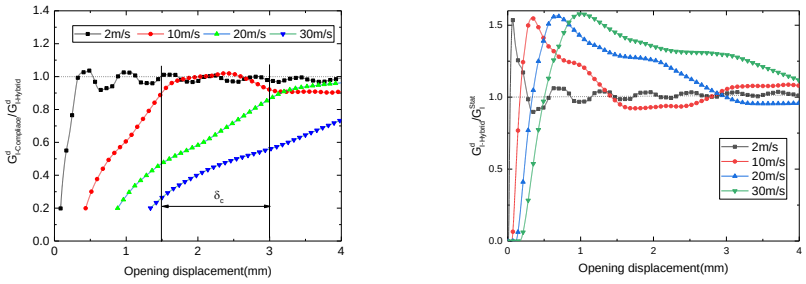

(**a**) (**b**)

Figure 6. (**a**)The difference between ERRs calculated by compliance method and hybrid method; (**b**) Energy release rate with various loading rate for ramped input.

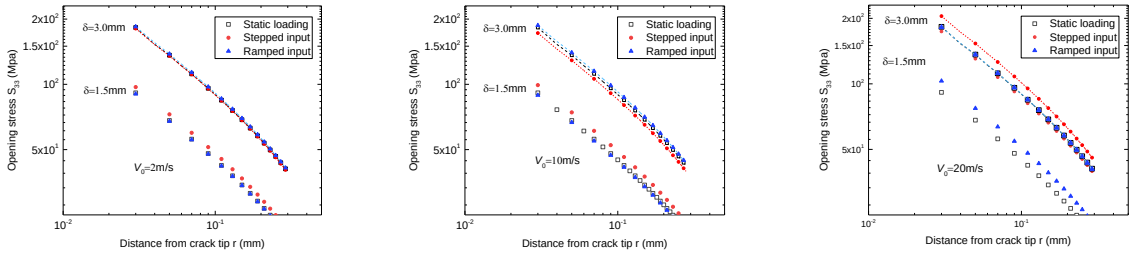

(**a**) (**b**) (c)

Figure 7. Opening stress distribution in the vicinity of the crack tip at the displacement rate (**a**) 2 m/s, (**b**) 10 m/s, (**c**) 20 m/s.

To explain the difference in Figure 6(a), the ERRs under different opening velocities are calculated and compared with the static ERR. It is shown that the value of ERR converges into the static value only when opening displacement rate equals to 2 m/s. As displacement rates increases, the difference between dynamic ERR and static ERR becomes larger. The opening stress, S_{33}, is plotted against the distance from the crack tip for ramped input and static loading, see Figure 7(a), (b) and (c). The intercept of opening stress represents the stress intensity factor. As shown in the figure, the opening stress distribution of stepped input loading is different from that of quasi-static loading

for loading velocities 2 m/s, 10m/s and 20 m/s. The opening stress distribution of ramped input loading is different from that of quasi-static loading when displacement rate is greater than 10 m/s.

4. Conclusions

The mode I dynamic fracture toughness of unidirectional carbon/epoxy laminates was loaded over a wide range of loading rates using DCB specimens. The following conclusions were obtained:

1. Dual electromagnetical Hopkinson bar system can guarantee pure mode I interlaminar fracture at high loading velocities in the range of 10–30 m/s.
2. A hybrid experimental-numerical method is developed to determine the fracture toughness. The compliance method underestimates the ERR under high-speed loading conditions.
3. The initiation fracture toughness under dynamic loading conditions is larger than its static value.

Acknowledgments: The authors acknowledge National Natural Science Foundation of China (Grant No. 11372256, 11527803 and 11772267) for financial support

Author Contributions: Huifang Liu, Chao Zhang and Yulong Li conceived and designed the experiments; Huifang Liu performed the experiments, analyzed the data and wrote the paper.

Conflicts of Interest: The authors declare no conflict of interest. The founding sponsors had no role in the design of the study; in the collection, analyses, or interpretation of data; in the writing of the manuscript, and in the decision to publish the results.

References

1. G.C. Jacob, J.M. Starbuck, J.F. Fellers, S. Simunovic, R.G. Boeman, The effect of loading rate on the fracture toughness of fiber reinforced polymer composites, Journal of applied polymer science 96(3) (2005) 899-904, https://doi.org/10.1002/app.21535. Available online: https://onlinelibrary.wiley.com/doi/abs/10.1002/app.21535 (24 February 2005),
2. M. May, Measuring the rate-dependent mode I fracture toughness of composites – A review, Composites Part A: Applied Science and Manufacturing 81 (2016) 1-12, https://doi.org/10.1016/j.compositesa.2015.10.033 Available online: https://www.sciencedirect.com/science/article/pii/S1359835X15003899 (30 October 2015),
3. G. Hug, P. Thévenet, J. Fitoussi, D. Baptiste, Effect of the loading rate on mode I interlaminar fracture toughness of laminated composites, Engineering Fracture Mechanics 73(16) (2006) 2456-2462, https://doi.org/10.1016/j.engfracmech.2006.05.019, Available online: https://www.sciencedirect.com/science/article/pii/S0013794406002098 (17 July 2006),
4. Standard D5528, Standard Test Method for Mode I Interlaminar Fracture Toughness of Unidirectional Fiber-Reinforced Polymer Matrix Composites1. ASTM International, West Conshohocken, PA, (2007).
5. H. Nie, T. Suo, B. Wu, Y. Li, H. Zhao, A versatile split Hopkinson pressure bar using electromagnetic loading, International Journal of Impact Engineering 116 (2018) 94-104, https://doi.org/10.1016/j.ijimpeng.2018.02.002, Available online: https://www.sciencedirect.com/science/article/pii/S0734743X17310084 (8 February 2018).